ATLAS High-Level Trigger performance for calorimeter-based algorithms in LHC Run-I

A Mann, on behalf of the ATLAS Collaboration

Ludwig-Maximilians-Universität München, Fakultät für Physik,
Am Coulombwall 1, 85748 Garching, Germany

E-mail: mann@cern.ch

Abstract. During Run-I of the Large Hadron Collider at CERN the ATLAS detector recorded more than $26\,\mathrm{fb}^{-1}$ of proton-proton collision events. One of the key components of the ATLAS detector is its trigger system. In order to keep up with the fast-paced evolution of the beam conditions during Run-I, the trigger selection had to be constantly adapted. For most of the calorimeter-based triggers only modest modifications of the thresholds had to be made, given the change in instantaneous luminosity of five orders of magnitude. This was achieved by various improvements in the High-Level Trigger algorithms, in several places abandoning the original RoI-based concept and introducing new features to overcome previous limitations. The excellent performance of both ATLAS and the LHC made possible the discovery of a new particle already during Run-I, the long-sought Higgs boson.

ATL-DAQ-PROC-2013-026
29 October 2013

1. Introduction

Run-I of the Large Hadron Collider (LHC) [1] comprises three data-taking periods in the years 2010 – 2012. During this time, more than $26\,\mathrm{fb}^{-1}$ of proton-proton collision data have been collected with the ATLAS detector [2]. The task of the ATLAS trigger and data-acquisition system (TDAQ) [3] is to reduce the initial event collision rate of up to 20 MHz during Run-I to the maximum storage rate of a few hundreds of events per second. Due to the very successful ramp-up of the instantaneous luminosity, the trigger algorithms had to be constantly adapted and improved in order to keep the rates within the limits given by the hardware constraints. The calorimeter-based triggers, selecting events with electrons, photons, taus, missing transverse energy ($E_{\mathrm{T}}^{\mathrm{miss}}$), or jets, are primarily based on information from the electromagnetic and hadronic calorimeters of the ATLAS detector. In addition, electron and tau triggers also use tracking information. The calorimeter-based triggers in particular had to cope with an increasing level of background activity from the increasing number of concurrent events (in-time pile-up). The present work describes the High-Level Trigger algorithms for these triggers[1], with focus on their performance and changes necessary in view of increasing in-time pile-up.

1.1. The ATLAS trigger system

The ATLAS trigger system is designed as a three-tiered system. The first level, Level 1 (L1), is hardware-based and runs on fast, custom-built electronics [5]. It uses coarse-grained information from the calorimeters and two types of fast-response muon chambers. During Run-I no track

[1] For a description of the ATLAS Level-1 calorimeter trigger cf. [4].

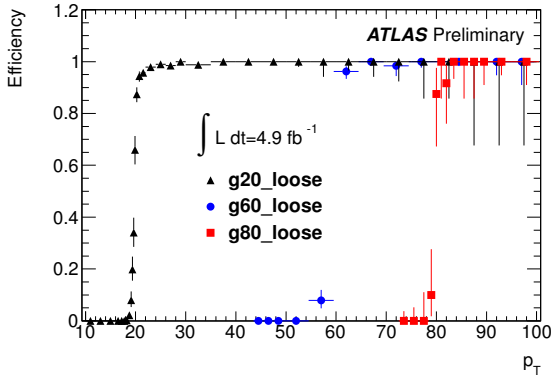

Figure 1. Efficiencies of photon triggers in 2011 relative to their respective L1 seeds as function of "tight" offline photon p_{T} [6].

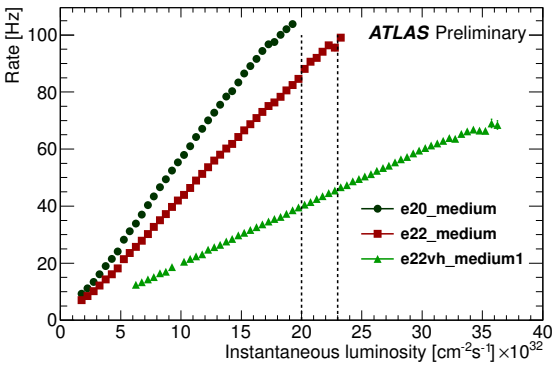

Figure 2. EF trigger rates for single-electron triggers in 2011, showing the achieved reduction of rates [6].

reconstruction and no topological cuts were affordable at this trigger level. L1 identifies regions of interest (RoIs), geometrical regions with significant detector activity, which are then passed as seeds to the next trigger level. Level 2 is software-based and runs on a dedicated computing cluster built from commercially available hardware. It fetches data from the RoIs at full detector granularity, and adds tracking and topological information. If an event is accepted at L2, event building (EB) is initiated and the event passed to the Event Filter (EF). Like L2, the EF is software-based and runs on its own dedicated computing cluster. It employs offline-like algorithms which have access to the full event information. L2 and EF are collectively called High-Level Trigger (HLT). Table 1 shows the evolution of important figures of merit for the ATLAS TDAQ and the LHC during Run-I.

Table 1. Evolution of important figures of merit for ATLAS and the LHC during Run-I

ATLAS TDAQ working point	Design	2010	2011	2012
Peak L1 output rate (kHz)	75	20	50	70
Peak L2 output rate (kHz)	3.5	3.5	5.5	6.5
EF output rate (kHz)	0.2	0.35	0.4	0.7
RoI data fraction (%)	2	5	5	10
Integrated luminosity (recorded, 1/fb)		0.045	5.08	21.3
LHC beam conditions	**Design**	**2010**	**2011**	**2012**
Center-of-mass energy $\sqrt{s}$ (TeV)	14	7	7	8
Peak average in-time pile-up	23 (avg.)	3	18	36
Peak instantaneous luminosity (Hz/cm^2)	10^{34}	$2.07 \cdot 10^{32}$	$3.65 \cdot 10^{33}$	$7.73 \cdot 10^{33}$
Peak number of proton bunches per beam	2808	348	1331	1380
Typical bunch spacing within a train (ns)	25	150	50	50

2. Performance of calorimeter-based High-Level Trigger algorithms during Run-I

2.1. Electron and photon triggers

The electron and photon trigger chains start from common seeds at L1, where no tracking information is available. The discrimination of electrons and photons from backgrounds at the HLT is based on cuts on a set of identification variables similar to those used offline: Shower

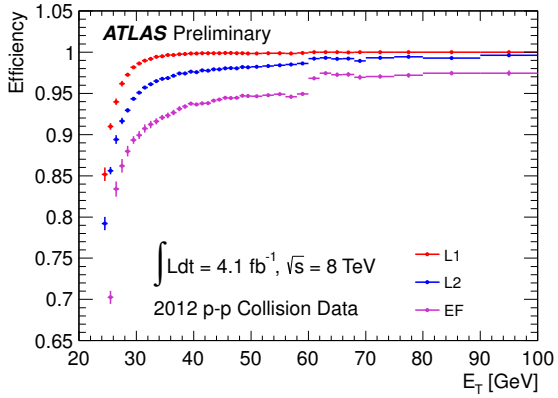

Figure 3. Efficiency of the logical OR of the primary single-electron triggers, e24vhi_medium1 + e60_medium1, for offline electrons with $E_{\mathrm{T}} > 25\,\mathrm{GeV}$ [7].

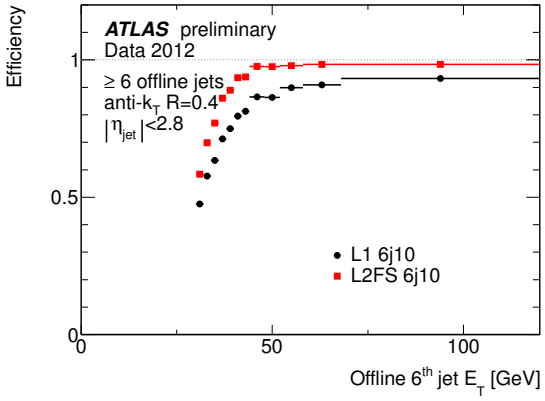

Figure 4. Efficiency of L1 and L2FS triggers in events with at least 6 offline anti-k_t $R = 0.4$ jets with $E_{\mathrm{T}} > 30\,\mathrm{GeV}$. L2FS recovers efficiency lacking at L1 in multijet events [8].

shape information is reconstructed from fine-granularity information from the calorimeters, and in addition tracking information is used to identify electrons. As supplementary triggers J/Ψ triggers and W tag & probe triggers for low transverse momentum (p_{T}) electrons and supporting triggers for background estimates are available.

The photon triggers had a very stable performance in both 2011 and 2012. They exhibit very sharp turn-on behavior and plateau efficiencies close to 100 % as is shown in Figure 1, independent of η and in-time pile-up[2]. The EF threshold of the lowest unprescaled photon trigger chain was raised from 60 to 80 GeV in 2011 and to 120 GeV for 2012.

For the lowest unprescaled electron trigger the EF threshold was raised from 20 to 22 GeV in 2011 and to 24 GeV for 2012. In addition in 2011 the L2 cuts defined in the "medium" and "tight" identification criteria were brought closer to the EF level selections and a "medium1" selection was deployed to adapt the trigger selection to the re-optimised offline selection for electrons with better performance under high pile-up conditions. Figure 2 shows the rate reduction achieved in 2011, where "vh" indicates a modified L1 seed [6]. In 2012 a pile-up robust track isolation was introduced and the identification cuts at the HLT were changed to improve pile-up robustness by cutting harder on pile-up insensitive quantities and looser on sensitive ones. Figure 3 shows the efficiency of the primary single-electron triggers used in 2012.

2.2. Jet triggers

Jet triggers scan for collimated energy deposits in the calorimeters arising from the hadronization of high-energy quarks or gluons. Jets are the most common final-state object at the LHC.

The original, entirely RoI-based design of the jet trigger suffered from the fact that only one jet could be reconstructed per RoI, leading to efficiency losses for events with many and near-by jets, and in general the discrepancy between trigger and offline algorithms used for jet finding. In 2010 the EF jet algorithms were running in pass-through mode, and so even before the activation of the EF for rejection of events at the beginning on 2011, the RoI-based algorithms at EF were replaced by a full-scan algorithm (EFFS), which finds jets independent of any L1 or L2 seed, but instead uses topological clusters as input to an anti-k_t algorithm. Similarly, the simplified cone algorithm at L2 was replaced in 2012 by a full scan (L2FS, also called L1.5). It applies an unseeded fast anti-k_t algorithm [9] to trigger towers with a granularity of $\Delta\eta \times \Delta\phi = 0.1 \times 0.1$

[2] η is pseudorapidity, ϕ the angle in the transverse plane of the coordinate system used by ATLAS [2].

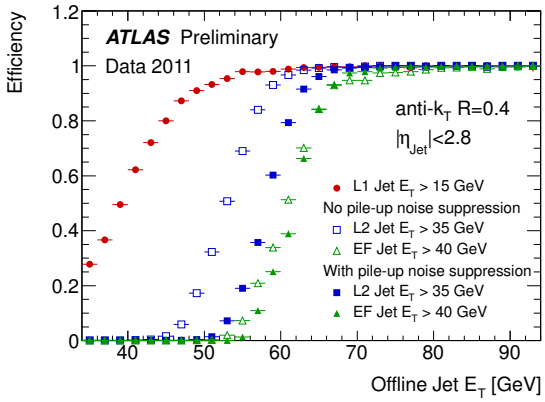

Figure 5. Comparison of the efficiency for a single jet trigger chain with and without noise suppression applied [8].

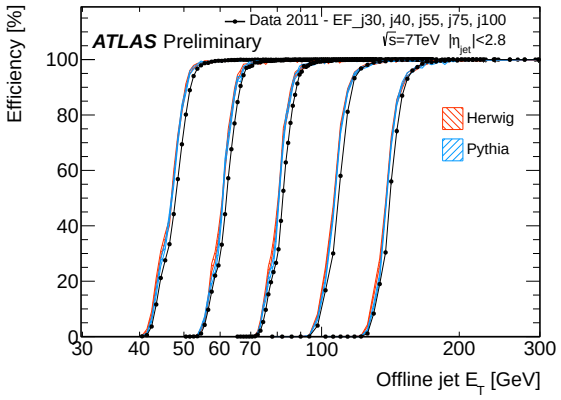

Figure 6. Efficiency for various Event Filter trigger chains calculated using the bootstrap method. [8].

because using cell-level granularity as input to jet finding is ruled out due to time constraints. This breaks the RoI concept, but is closer to the offline selection and thereby solves the problem of inefficiencies for multi-jet topologies and close-by jets as can be seen in Figure 4. Starting in May 2011 two-sided configurable cuts at cell-level were introduced, taking into account measured noise from pile-up and calorimeter electronics. This leads to a significant improvement at L2 as shown in Figure 5. The overall 99 % efficiency point is improved by about 5 GeV. The effect at EF is smaller because topological clustering already includes noise suppression. Figure 6 shows the EF efficiency for single jet triggers in 2012 computed with respect to events taken by a L2 trigger at 100 % efficiency. The improvements also made possible in 2012 to introduce efficient triggers on the sum of the p_{T} of all identified jets (H_T) and boosted topologies with wide energy deposits not well contained in single RoIs.

2.3. E_T^{miss} triggers

The $E_{\mathrm{T}}^{\mathrm{miss}}$ triggers are designed to select collision events with non-interacting particles, identified as a significant imbalance in the vectorial sum of all particle energies transverse to the beam axis[3]. Being a global sum over the full calorimeter, this trigger is very susceptible to pile-up effects. An increase of in-time pile-up leads to an increase of the average energy deposited in the calorimeter and thus also in measurement fluctuations. This causes strong non-linearities in the rates of low-threshold $E_{\mathrm{T}}^{\mathrm{miss}}$ triggers as function of luminosity as can be seen in Figure 7, and presents a challenge for the trigger type. Algorithms and noise thresholds need to be carefully tuned to allow for a separation of different types of $E_{\mathrm{T}}^{\mathrm{miss}}$, real $E_{\mathrm{T}}^{\mathrm{miss}}$ from invisible particles and fake $E_{\mathrm{T}}^{\mathrm{miss}}$ from pile-up and resolution effects.

In 2011 the value of $E_{\mathrm{T}}^{\mathrm{miss}}$ used at L2 was equivalent to that computed at L1, and thus the $E_{\mathrm{T}}^{\mathrm{miss}}$ trigger at L2 suffered from the poor resolution of the L1 measurement. A substantial improvement was achieved after an upgrade of the calorimeter readout in 2012 and the introduction of a parallel line of data access. This allowed for a fast recomputation of $E_{\mathrm{T}}^{\mathrm{miss}}$ at L2 from cell-based sums of E_{T} provided by the calorimeter front-end boards, giving a much better resolution than the trigger-tower based $E_{\mathrm{T}}^{\mathrm{miss}}$ of L1. At EF level, the cell-based algorithm was replaced in 2012 by a new algorithm summing calibrated topological clusters instead, which also applies a local weight calibration for the cell energies [10]. Figure 8 shows a comparison of the

[3] Muon information is available at both L2 and EF, but was not included in the $E_{\mathrm{T}}^{\mathrm{miss}}$ computation in active 2011 triggers, and in 2012 only in one combined chain at EF level.

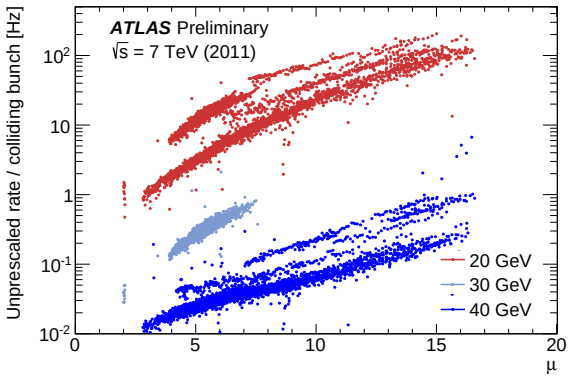

Figure 7. Rates per bunch crossing for low-threshold $E_{\mathrm{T}}^{\mathrm{miss}}$ triggers in 2011 as function of the number of concurrent interactions μ, illustrating the stronger-than-linear increase of the rates as function of in-time pile-up [11].

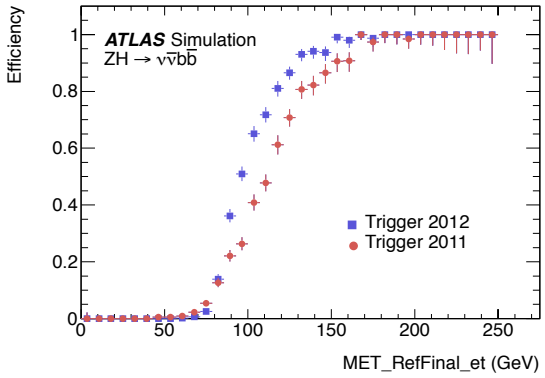

Figure 8. Efficiency of the lowest unprescaled $E_{\mathrm{T}}^{\mathrm{miss}}$ trigger chains in 2011 (thresholds: 50, 55, 60 GeV at L1, L2, EF) and 2012 (40, 45, 80 GeV, using topological clusters with local weight calibration at EF) [11].

efficiency of the $E_{\mathrm{T}}^{\mathrm{miss}}$ trigger in simulated $ZH \to \nu\nu b\bar{b}$ events for the lowest unprescaled chains in 2011 and 2012. Despite the harsher pile-up conditions in 2012, looser trigger requirements than in 2011 could be afforded, and the acceptance is considerably improved. Another important development was the introduction of a new type of trigger in 2011, the $E_{\mathrm{T}}^{\mathrm{miss}}$ significance (XS) triggers. They exploit the different scaling behavior of fake and real $E_{\mathrm{T}}^{\mathrm{miss}}$ with $\sum E_T$, the scalar sum of the transverse energies of all particles, and allow to accept events with real $E_{\mathrm{T}}^{\mathrm{miss}}$ below the $E_{\mathrm{T}}^{\mathrm{miss}}$ trigger thresholds.

2.4. Tau triggers

The tau triggers select hadronic decays of tau leptons, which are identified as collimated energy deposits in the calorimeters accompanied by one or a low number of matching charged tracks. Similar to the electron and photon triggers, the HLT tau algorithms accept events based on selection cuts on tracking and calorimeter-based variables, where the EF tries to be as close as possible to the offline selection. The HLT tau algorithms have been run in pass-through mode (i. e. not rejected events) until mid of 2010.

For 2011, several aspects of the cut-based selection at L2 and EF were improved and modified to bring it closer to the offline selection: At L2 the geometrical window around the RoI was enlarged from 0.6×0.6 to 0.8×0.8, noise thresholds at cell level were introduced, and the definition of the EM radius variable, one of the selection variables, was changed to match the offline definition. At EF level, a tighter track selection and more shape variables were used, in addition shape variables were made dependent on the transverse energy of the tau candidate, and the tau energy was now computed from topological clusters at a local calibration scale [12].

Plotting the efficiency of the tau trigger as function of the number of pile-up interactions a severe performance degradation for events with high in-time pile-up was observed in 2011 as shown in Figure 9. Several adjustments in the computation of the identification variables at L2 were thus done for 2012: The cone size used to compute the L2 EM radius, the energy-weighted shower radius of the L2 tau candidate, was reduced from 0.4 to 0.2. An additional cut was introduced to restrict tracks being used in the L2 tau identification to those which have an impact parameter compatible with that of the highest-p_{T} track, $|\Delta Z_0| < 2\,\mathrm{mm}$. Also the track-based isolation was complemented by a calorimeter-based isolation cut. At EF level, the cut-based selection was replaced in 2012 by a multi-variate algorithm based on boosted-

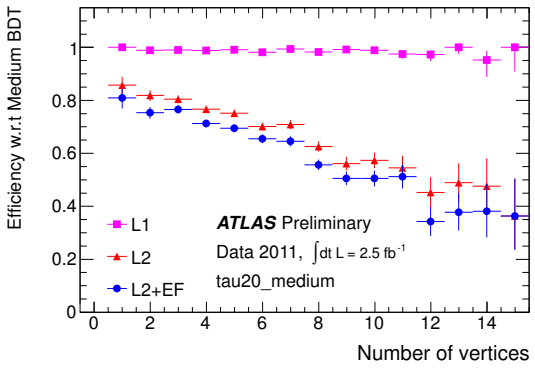

Figure 9. Efficiency of the cut-based trigger selection measured in 2011 data [13].

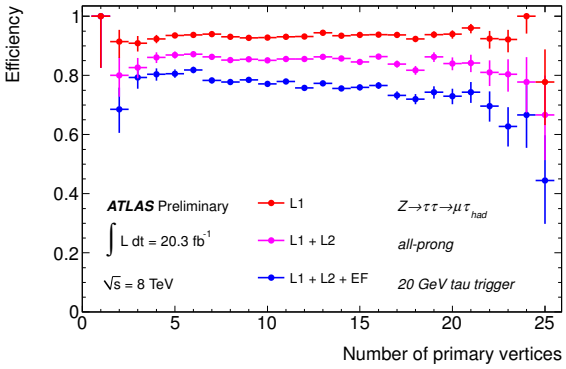

Figure 10. Efficiency of the BDT-based trigger selection measured in 2012 data [13].

decision trees (BDT). Figure 10 shows the efficiency of a 20 GeV tau trigger for offline taus with $p_{\mathrm{T}} > 30$ GeV measured in 2012 data, demonstrating the pile-up robustness achieved by the improved trigger selection at L2 and EF.

3. Ideas and prospects for Run-II

In Run-II of the LHC, foreseen for 2015 – 2018, the center-of-mass energy is expected to be raised to 13 TeV and the instantaneous luminosity to possibly exceed the design value of 10^{34} Hz/cm^2. Improvements of the ATLAS TDAQ system planned for Run-II include a new L1 Topological processor allowing to use topological cuts not only at the HLT but also at L1, and a new FastTracker, a hardware-based tracking system, which provides the HLT with track parameters for the full event and could be used to reconstruct primary vertices, giving an event-by-event estimate of pile-up. A network upgrade and new read-out systems will allow a higher data access rate, and L2, EB and EF will be merged, yielding a unified HLT architecture [14]. The output rate of L1 will be increased from 70 to 100 kHz and the final storage rate up to 1 kHz.

The trigger strategy for Run-II will benefit from the TDAQ upgrades, but algorithms and calibrations will still need to become even more pile-up robust, and isolation requirements to be revisited to avoid inefficiencies. Like the tau triggers, the electron and photon triggers could switch to multi-variate algorithms. In general, all triggers will have to move to tighter selections and try to be closer to the offline selection, making sure that there is a versatile, efficient and unbiased set of signal and background triggers for Run-II.

References

[1] Evans L and Bryant P 2008 *JINST* **3** S08001
[2] ATLAS Collaboration 2008 *JINST* **3** S08003
[3] ATLAS Collaboration CERN-LHCC-2003-022 http://cds.cern.ch/record/616089
[4] Achenbach R *et al.* 2008 *JINST* **3** P03001
[5] ATLAS Collaboration CERN-LHCC-98-014 http://cds.cern.ch/record/381429
[6] ATLAS Collaboration ATLAS-CONF-2012-048 http://cds.cern.ch/record/1349309
[7] https://twiki.cern.ch/twiki/bin/view/AtlasPublic/EgammaTriggerPublicResults
[8] https://twiki.cern.ch/twiki/bin/view/AtlasPublic/JetTriggerPublicResults
[9] Cacciari M and Salam G P 2006 *Phys. Lett.* **B641** 57–61 (*Preprint* hep-ph/0512210)
[10] Hristova I ATL-DAQ-PROC-2012-051 http://cds.cern.ch/record/1485638
[11] https://twiki.cern.ch/twiki/bin/view/AtlasPublic/MissingEtTriggerPublicResults
[12] ATLAS Collaboration ATLAS-CONF-2013-006 http://cds.cern.ch/record/1510157
[13] https://twiki.cern.ch/twiki/bin/view/AtlasPublic/TauTriggerPublicResults
[14] Kama S ATL-DAQ-PROC-2012-061 http://cds.cern.ch/record/1494175